AAS 93-164

# *IN-SITU* RADIO-METRIC TRACKING TO SUPPORT NAVIGATION FOR INTERPLANETARY MISSIONS WITH MULTIPLE SPACECRAFT

Robert D. Kahn*, Sam W. Thurman†, and Charles D. Edwards‡

Doppler and ranging measurements between spacecraft can be obtained only when the ratio of the totat received signal power to noise power density ($P_t/N_0$) at the receiving spacecraft is sufficiently large that reliable signal detection can be achieved within a reasonable time period, In this paper the requirement on $P_t/N_0$ for reliable carrier signal detection is calculated as a function various system parameters, including characteristics of the spacecraft computing hardware and *a priori* uncertainty in spacecraft-spacecraft relative velocity and acceleration, Also calculated is the $P_t/N_0$ requirement for reliable detection of a ranging signal, consisting of a carrier wrth pseudo-noise phase modulation. Once the $P_t/N_0$ requirement is determined, then for a given set of assumed spacecraft telecommunication characteristics (transmitted signal power, antenna gains, receiver noise temperatures) it is possible to calculate the maximum range at which a carrier signal or ranging signal may be acquired. For example, if a Mars lander and a spacecraft approaching Mars are each equipped with 1-meter diameter antennas, the transmitted power is 5 Watts, and the receiver noise temperatures are 350 K, then S-Band carrier signal acquisition can be achieved at ranges exceeding 10 million kilometers.

A brief error covariance analysis has been conducted to illustrate the utility of *in situ* Doppler and ranging measurements for Mars approach navigation. The results indicate that navigation accuracies of a few kilometers can be achieved with either data type, The analysis also illustrates dependency of the achievable accuracy on the approach trajectory velocity .

## INTRODUCTION

In recent years there has been increased interest in pursuing an intensive program of lunar and Mars exploration with robotic and piloted spacecraft. Conducting an expansive program of lunar and Mars exploration with multiple spacecraft will present new technical and operational challenges. Future missions to Mars may rely on aerobraking to achieve orbit insertion. The aerobraking technique reduces a spacecraft's propellant requirement, but imposes more stringent navigation constraints than have been needed for previous interplanetary missions. Simultaneous deployment of a large number of spacecraft at the Moon and/or Mars could place unprecedented demands on already taxed ground-based tracking resources. The need for greater navigational accuracy and the need to relieve the burden on ground-based antennas could both be addressed by making use of *in-situ* radio-metric tracking measurements. Doppler and ranging measurements between spacecraft provide navigation information complementary to Earth-based techniques, and could potentially decrease reliance on ground-based tracking.

This paper investigates requirements for successful acquisition of *in-situ* radio-metric data types, and discusses potential measurement precision. An error covariance analysis has also been performed to investigate. the navigation accuracy that can be

* Member, Technical Staff, Tracking Systems and Applications Section, Jet Propulsion Laboratory
† Technical Manager, Navigation Systems Section, Jet Propulsion Laboratory
‡ Technical Group Supervisor, Tracking Systems and Applications Section, Jet Propulsion Laboratory

achieved using Doppler and ranging measurement% between a spacecraft approaching Mars and a Mars-orbiting satellite used as a navigation aid. The analysis was designed to build upon the results of similar studies conducted previously[1-4]. The error covariance analysis points out some of the most important trajectory and tracking system parameters that influence the navigation performance that can be obtained, While the mission scenario studied herein is for the planet Mars, *in situ* radio tracking is also applicable to lunar spacecraft navigation as well, or to any other mission in which a radio beacon or another spacecraft is available near the target body and can be used as a navigation aid.

## CARRIER SIGNAL ACQUISITION

To perform *in-situ* Doppler measurements, one spacecraft tracks the phase of a carrier signal transmitted from a second spacecraft. If the measurement is one-way, the signal originates at the second spacecraft; in a two-way measurement, the signal is uplinked by the first spacecraft, coherently transponder by the second spacecraft, and then phase-tracked by the first spacecraft. The Doppler shift on the. received signal provides a direct measure of the relative line-of-sight velocity of the two spacecraft. While. one-way measurements are. more easily implemented, they are inferior to two-way measurements because an unknown frequency offset between the two spacecraft oscillators can cause a significant error in the inferred relative. velocity of the spat.ecrafl.

### Detection Strategy

A simple signal detection strategy is depicted in Fig. 1, The incoming signal is mixed with a locally generated model, the resulting baseband signal is integrated for T seconds, and N consecutive T-second integrations are Fourier transformed. The resulting Fourier coefficients reflect signal or noise amplitude in N bins of width I/(N"l") Hz, centered at the model frequency (Fig. 2). In general, the a priori uncertainty of the signal frequency, Av, will be larger than the frequency range, 1/T Hz, which can be searched with a single Fourier transform, so a number of different model frequencies will have to be tried before the signal is detected.

To determine whether the signal is present in a given frequency span (the range of frequencies probed by a single Fourier transform) an amplitude detection threshold is selected. It is desirable. to have the threshold be sufficiently low so that the. signal will almost always be detected when it is present, and sufficiently high so that noise. will not often be mistaken for signal. If the amplitude in some Fourier resolution bin exceeds the. threshold, then the same frequency model is used to process the next NT seconds of data. If signal is detected in the same bin in two consecutive Fourier transforms, then it is assumed that the true signal has been found, and phase-lock-loop tracking commences.

Note that in any given Fourier transform, it is possible that the noise amplitude in at least one Fourier resolution bin will exceed the amplitude, detection threshold. If we require 99% confidence of detecting the true signal twice consecutively when it is present, and 1% probability of mistaking noise for signal, we obtain a relation between N and $(P_t/N_0)T$ which is approximated by: $(P_t/N_0)T = 29\ N^{-0.92}$. The appendix discusses how this equation is obtained,

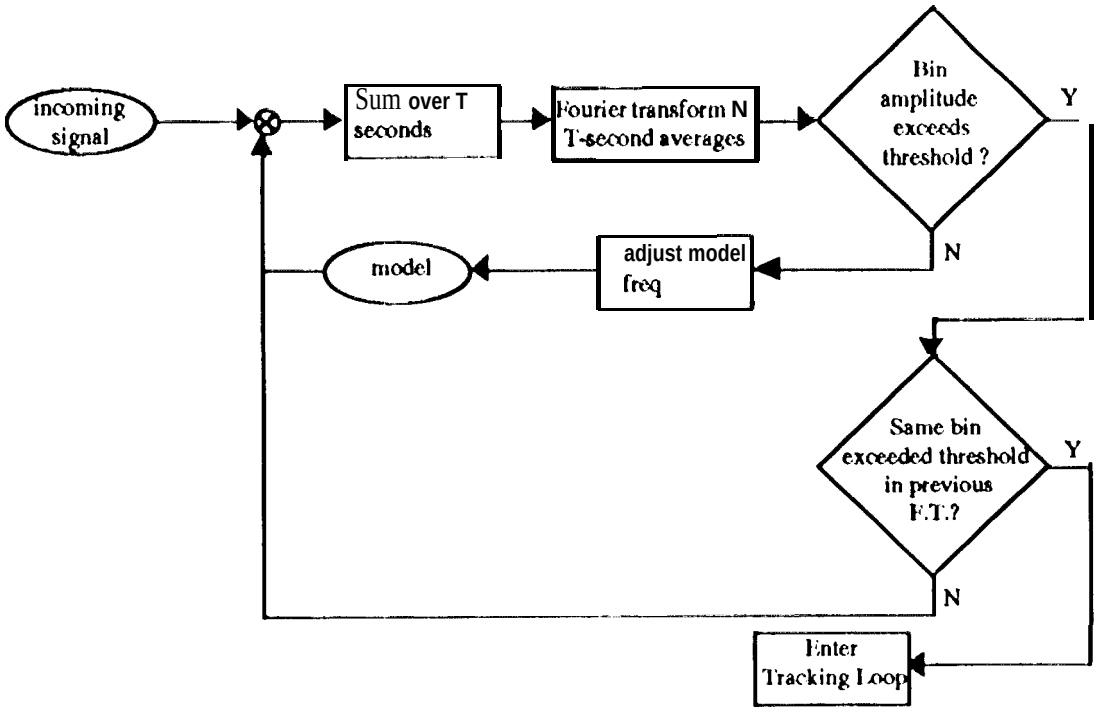


**Fig. 1 A simple carrier signal detection strategy**

If the signal is equally likely@ lie anywhere. within the search space, **Av,** then the mean time to signal acquisition is $T_{ACQ} \approx$ Av $NT^2/2$ (Ref. 4). The acquisition time is proportional to NT because. that is the time required to accumulate data for each Fourier transform, and is proportional to TAv because the frequency search space contains $T\Delta v$ spans of width (1/T) Hz.

Taken together, the equations $(P_t/N_0)T = 29\,N^{-0.92}$ and $\bar{T}_{ACQ} \approx$ Av $NT^2/2$ imply that for a given value of either N, T, or NT, there. is a functional relationship between $\bar{T}_{ACQ}/\Delta v$ and the minimum $P_t/N_0$ required for reliable signal acquisition (99% Confidence of signal detection and 1 % probability of false alarm). The contours in Fig. 3 illustrate these relationships. As an example, if N = 1000 and T = 0.01 second, it is required that $(P_t/N_0) \geq 7$ dB-Hz. The cm-responding value of $\bar{T}_{ACQ}/\Delta v$ is about 0.05 see/Hz; e.g. for a frequency uncertainty of 1 kHz, the expected search duration is 50 seconds.

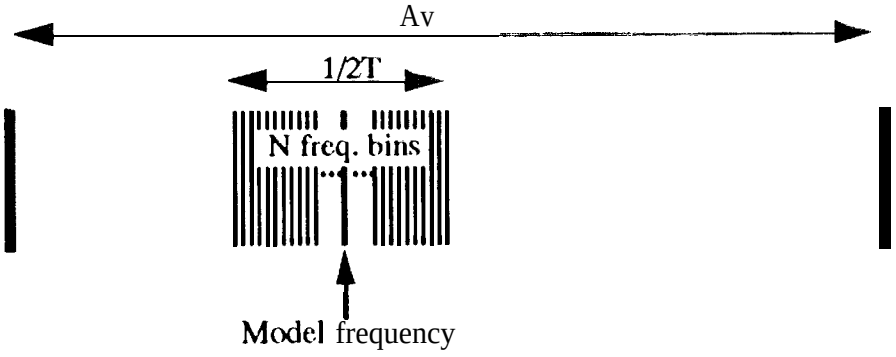


**Fig. 2 Relationship between frequency search range, Av Hz, and frequency span, 1/2T Hz, probed by a single Fourier transform**

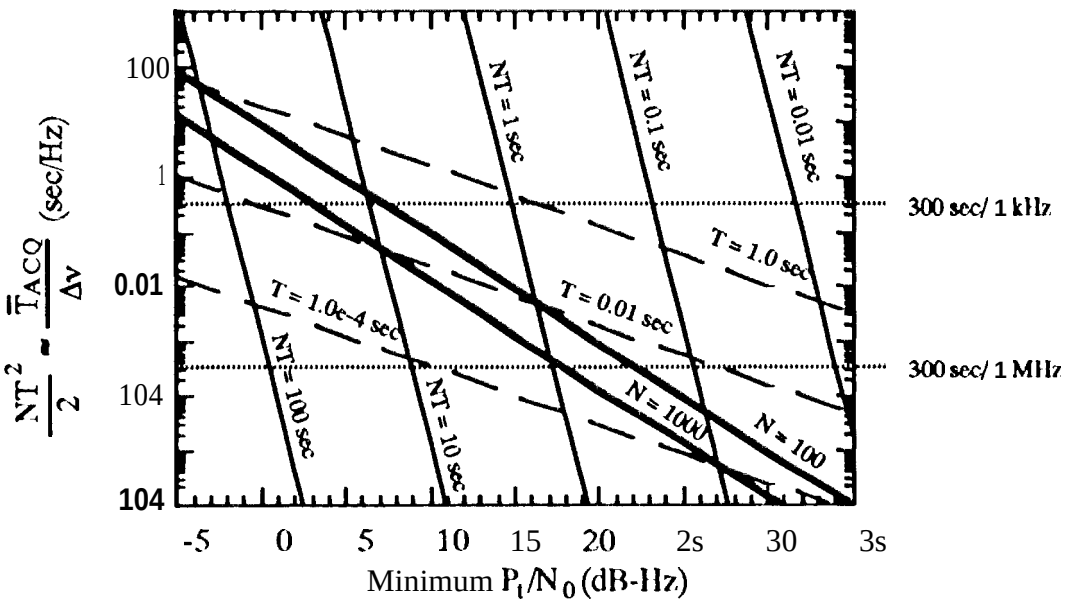


**Fig. 3 Relationships between $\bar{T}_{ACQ}$ /Av, N, T, and the minimum $P_t/N_0$ required to ensure that $P_{false}$= 0.01 while $P_{detect}$ = 0.99.**
**— Carrier signal detection —**

Fig. 3 suggests that no matter what the search range, Av, it is always possible to specify N and T such that (1) the requirement on $(P_t/N_0)$ is arbitrarily small, and (2) the search time, $\frac{NT^2\Delta v}{2}$, is arbitrarily short. In practice, however, there are constraints due to both spacecraft dynamics and hardware (and perhaps software) which impose restrictions on the allowable values of N, T, and their product, NT.

Constraints on the Selection of N and T. Hardware on board the spacecraft dictates a maximum value of N and a minimum value for T. At present, Fourier transform chips which can operate on hundreds of points are commonplace. If N is constrained by hardware to be at most 1024, then the data dump interval, T, is greater than $10^{-4}$ sec over most of the range of $P_t/N_0$ in Fig. 3. A dump rate, 1/T, of 10,000 Hz is well within the capabilities of existing ground-based hardware., and may be feasible for space-qualified systems by the late 1990's.

Constraints on data collection interval, NT. Constraints on the product NT result from unmodelled beacon accelerations and from oscillator drift, both of which cause the frequency, f, of the received signal to change in time. Signal detection can be severely impeded if the signal moves through multiple. Fourier resolution bins over the time, NT, during which the data for a single Fourier transform are acquired, We will require that the change in frequency due to an unmodelled acceleration, $\delta a$, over time NT be smaller than 1/(2NT) Hz (half the size of one Fourier resolution bin). This condition is satisfied when

$$NT \le \sqrt{\frac{c}{2f\,\delta a}}\,. \tag{1}$$

Similarly, we require that the change. in frequency due to oscillator instability over the time NT be smaller than 1/(2NT) Hz. If $\sigma_{y_i}(NT)$ is the Allan standard deviation of spacecraft i's oscillator, then

$$NT < \frac{1}{2f\sqrt{\sigma_{y_1}^2(NT)+\sigma_{y_2}^2(NT)}} \qquad (2)$$

Contours corresponding to NT = 10" for n = -2 to 2 are plotted in Fig. 3.

Range of Frequencies to be Searched, $\Delta v$. The range of frequencies to be searched, $\Delta v$, is a function of the uncertainty in spacecraft-spacecraft relative velocity. Also, for one-way transmission (and for the uplink of a two-way measurement), Av depends on an unknown frequency offset in the transmitting spacecraft's reference oscillator.

If the spacecraft-spacecraft velocity uncertainty is $\delta v$, the corresponding uncertainty in carrier frequency is:

$$Av = f\,(\delta v/c)$$

The day-to-day drift in carrier frequency due to oscillator instability depends on the quality of the spacecraft oscillator. If the oscillator is not temperature-stabilized, an S-Band (2.3 GHz) carrier frequency may vary by thousands of Hz. A highly stable oscillator has day-to-day variations much smaller than 1Hz at S-Band.

Example: Calculation of $P_t/N_0$ Requirement for Carrier Acquisition. The above information may be combined in order to calculate the $P_t/N_0$ requirement for reliable carrier acquisition,

As an example, suppose one spacecraft is fixed on the surface of a Mars, while a second spacecraft is on approach to Mars. The spacecraft are equipped to transmit and receive at S-Band. It is desired that a carrier signal be acquired within S minutes. Neither spacecraft has *a priori* knowledge of the spacecraft-spacecraft relative velocity and acceleration.

Since the spacecraft have no *a priori* knowledge of their relative velocity, the range of frequencies to be searched, Av, is the full spacecraft-spacecraft relative velocity. A typical Mars approach velocity is 4 km/see, corresponding to a frequency search range of approximately 31 kHz at S-Band. Since 5 minute acquisition is desired, it is required that $T_{ACQ}/\Delta v \lesssim 0.01$ sec/Hz.

The relative acceleration of the lander and approach spacecraft is principally due to Mars rotation, which imparts up to 0.017 $m/s^2$ of acceleration to the lander, This unmodelled acceleration imposes the constraint NT $\leq$ 2 sec. Eq. (2) indicates that the upper bound on NT arising from oscillator stability is also 2 sec if the 2-second AlIan standard deviation of the spacecraft oscillators is smaller than $8 \times 10^{-11}$ see/see.

If the desired time to signal acquisition is S minutes, then the parameter constraint.. may be summarized as follows:

| *Constraint* | *Reason* |
|---|---|
| $T_{ACQ}/\Delta v \lesssim 102$ see/I Iz | 5 min. acquisition, Av = 31 kHz, |
| NT< 2 sec | Eq. (1) (unmodelled accel.) |

The constraints $T_{ACQ}$ /Av $\lesssim$ 0.01sec/Hz and NT $\leq$ 2 sec are represented by the unshaded region in Fig, 4. The minimum $P_t/N_0$ satisfying both constraints is approximately 13 dB-Hz.

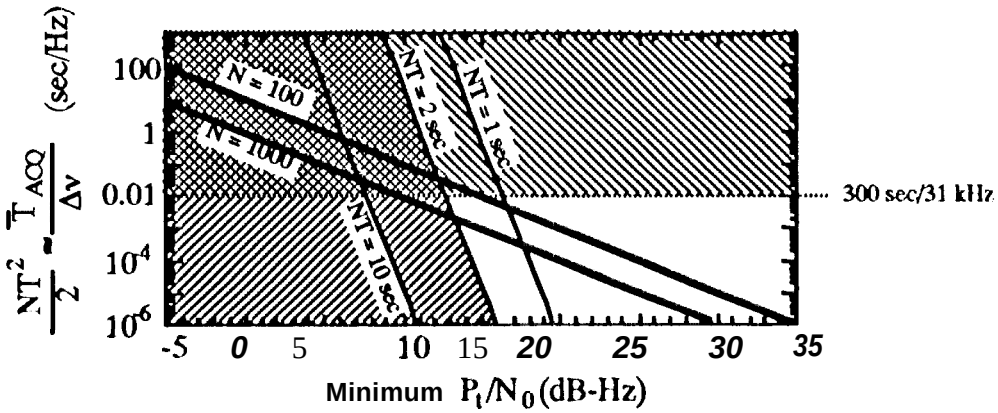


Fig. 4 **Given the constraints NT ≤ 2sec and $T_{ACQ}/\Delta\nu \leq 0.01$ sec/Hz, the minimum $P_t/N_0$ needed for reliable carrier detection is 13 dB-Hz**

Once the $P_t/N_0$ requirement is known, then if the. spacecraft telecommunication characteristics are specified, one can determine the maximum range at which the carrier can be acquired. Fig. 5 illustrates $P_t/N_0$ as a function of range between the Mars lander and approach spacecraft, for several different assumptions about the spacecraft telecommunications system. The tapering of the curves at smaller ranges is due. to the increasing contribution of Mars to the system noise temperature.

## DOPPLER MEASUREMENT PRECISION

Once a carrier signal has been detected, tracking the signal's phase is straightforward. Phase tracking precision depends on a variety of factors including $P_t/N_0$ and oscillator stability. However, if the carrier can be tracked at all, then the point-to-point phase precision is much smaller than one RF cycle (e.g. 13 cm at S-Band), Phase tracking precision does not significantly affect the accuracy with which the Mars approach spacecraft's state can be determined by fitting to an arc of beacon-spacecraft Doppler data. Determination of the approach spacecraft's state should be limited by other effects, such as unmodelled spacecraft acceleration%.

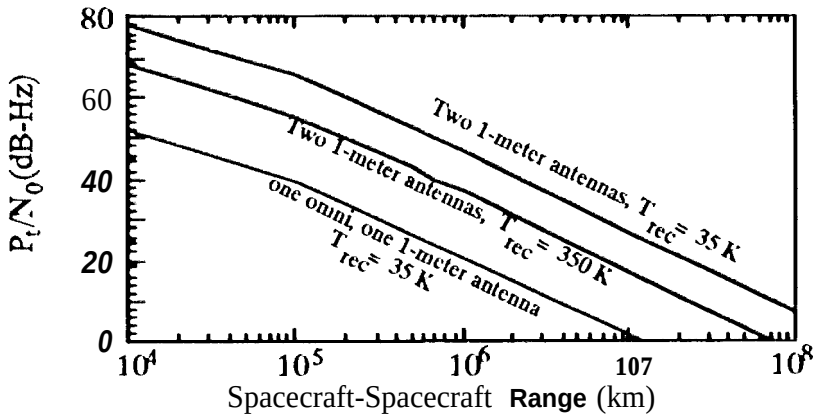


**Fig. 5 $P_t/N_0$ as a function of Mars lander-approach spacecraft range. Transmitted power is 5 W.**

## RANGING SIGNAL ACQUISITION

### Signal Structure

The ranging measurement is performed as follows: A spacecraft transmits a signal to a second spacecraft which locks on to the signal and coherently transponds it back to the first spacecraft, Two-wa y ranging offers the tremendous advantage of elim inating the problem of unknown spacecraft clock offsets which can significantly degrade the accuracy of a one-way measurement. However, the accuracy of the two-way measurement is still affected by the first spacecraft's clock instability over the round-trip light time, For example, if the spacecraft oscillator has Allan variance of $10^{-11}$ see/see over time scales of minutes and the two-way light time is 100 seconds (30 million km), then clock instability introduces a 30 cm error.

Assume a ranging signal of the following form:

$$s(t) = A \cos(\omega_0 t + \beta PN(p, f_c, t-t_n) + \phi_0),$$

where

| | |
|---|---|
| A | is the. signal amplitude |
| $\omega_0$ | is the carrier frequency |
| $\beta$ | is the modulation index, $0 < \beta < \pi/2$ |
| PN | is a pseudonoise sequence with period p and chip rate $f_c$ |
| p | is the period of the PN sequence |
| $f_c$ | is the chip rate of the PN sequence, i.e. $1/f_c$ is the chip duration, $\tau_c$, |
| $t_n$ | is the epoch of the PN sequence |
| $\phi_0$ | is the phase of the carrier signal at t = O |

Pseudonoise (PN) sequences[5] are a special class of sequences of 1's and –1's which can be generated by linear feedback shift registers. Individual elements of such a sequence will be referred to as "symbols". PN sequences are periodic; a given sequence consists of repetitions of a symbol pattern of length p. For every integer n, there exists at least one pseudonoise sequence of period 2" -1. If r(j) is a PN sequence with period p, then the autocorrelation of r(j), $R_p(i) = (1/p)\int_{i}^{p} r(j)\, r(j+i)\, dj$, is equal to 1 for i = any integer multiple of p, and is equal to -l/p for all other i (Fig. 6). The chip rate, $f_c$, of a PN sequence is the rate at which symbol transitions occur.

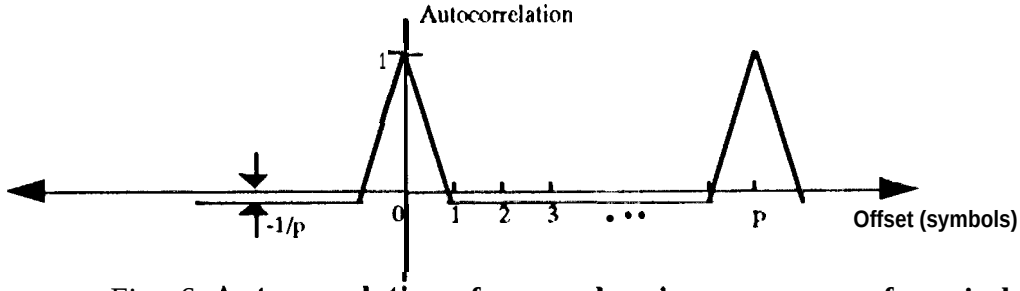


Fig. 6 **Autocorrelation of a pseudonoise sequence of period p.**

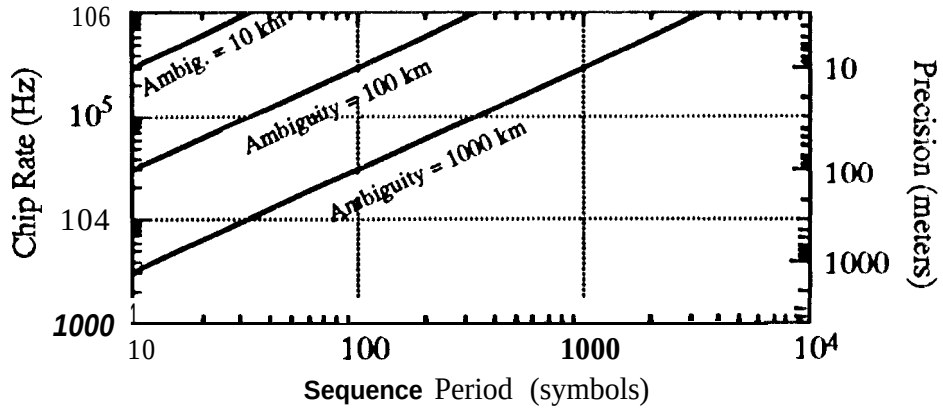


**Fig. 7 Relationship between chip rate, length of PN sequence, range ambiguity, and ranging measurement precision (assumed tracking error is 1 % of' chip length).**

During a two-way ranging measurement, the spacecraft originating the PN signal simultaneously receives a PN code which had been transmitted one round-trip-light-time earlier. The incoming PN code is offset from the. current state of the uplink code by an amount equal to the round-trip-light-time divided by the chip duration, $\tau_c$. This code offset can be determined by cross-correlating the received signal with the locally generated sequence, To ensure that such a two-way ranging measurement is unambiguous, it is required that the period of the PN sequence, $p\tau_c$, be larger than the a *priori* uncertainty in the spacecraft-spacecraft range. The relationship between the chip rate, PN period, and range ambiguity is plotted in Fig. 7. The ranging precision is proportional to the product of the chip duration and the precision with which the PN sequences can be aligned. If chip alignment precision of 1% can be achieved in the tracking loop, then a chip rate of 1 MHz corresponds to a ranging measurement precision of 3 meters.

## Ranging Signal Detection

The incoming signal is

$$s(t) = A \cos(\omega_0 t + \beta PN(p, f_c, t-t_n) + \phi_0)$$

and the locally-generated model for the carrier is

$$\tilde{s}(t) = \exp[i\,(\tilde{\omega}_0 t + \beta PN(p, \tilde{f}_c, t-\tilde{t}_n))\,]$$

If the carrier i.. fully suppressed ($\beta = \pi/2$), then multiplication of the signal and model, followed by low-pass filtering yields the following:

$$C(t) = s(t) \times ;(t) = A/2 \;\exp[i\,((\tilde{\omega}_0-\omega_0)t - \phi_0))\,] \times PN(p, f., t-t_n)\, PN(p, \tilde{f}_c, t-\tilde{t}_n)$$

In general, three model parameters must be determined. However, it is possible to design the spacecraft so that the pseudonoise clock and the transmitted carrier frequency are both referenced to the same frequency standard. In this case, a search must be conducted only for $\omega_0$ and $t_n$; the code frequency, $f_c$, is a deterministic function of the carrier frequency, $\omega_0$.

The product of actual and model signals is integrated over T-second intervals, and a set of N consecutive integrations is Fourier transformed, It is important that the time period NT be long enough that the product PN(p, $f_c$, t-$t_n$)×PN(p, $\tilde{f}_c$, t-$\tilde{t}_n$) approximates the PN autocorrelation function. The signal can be detected via the Fourier transform only when 1) the model frequency lies within l/2T Hz of the actual frequency, and 2) the. difference between the model PN epoch and the true PN epoch is a fraction of a chip.

Since a given Fourier transform probes a region of frequency space of width 1/T Hz, centered at the model frequency, a total of TAv Fourier transforms are requrired to search a frequency range of Av Hz, Note, however, that a T-second average of {signal x model} suffers an amplitude loss equal to sinc($T(\tilde{\omega}_0-\omega_0)/2$) (Ref. 7); if the signal and model differ by 1/2T Hz, the corresponding loss in amplitude is about 2 dB. It may be advantageous, therefore, to space the frequency models by an amount $1/k_fT$ ($k_f$> 1) to reduce the distance between the signal and the best model frequency. Reducing the spacing between frequency models increases the number of models needed to cover the search space,

Even if the model frequency is perfect, a fully suppressed carrier cannot be detected unless **the model PN epoch is also close to truth (within a fraction of a chip). If the model** PN epoch is stepped in single-chip increments, then the best PN code alignment achieved may be off by as much as 1/2 chip, resulting in an amplitude loss of 3 dB (see Fig. 6). In order to decrease the potential loss of amplitude due to fractional PN-code misalignment, one may conduct the search using smaller step sizes, at the cost of requiring additional models to cover the entire search space. If the step size is $1/k_c$ chip, then up to $k_c$ x p offsets may need to be tested before the signal is detected.

The signal search space is illustrated in Fig. 8, for the case $k_f$ = 1. The search space consists of $N_f$ x $N_s$ cells, where $N_f$ is the number of model frequencies and $N_s$ is the number of trial symbol offsets. Each Fourier transform of {signal x model} probes a range of (l/T) Hz, centered at the model frequency. One method of performing a systematic search is to step through all possible model symbol offsets for a given model frequency. If the signal is not detected, the model frequency is then shifted by 1/T Hz.

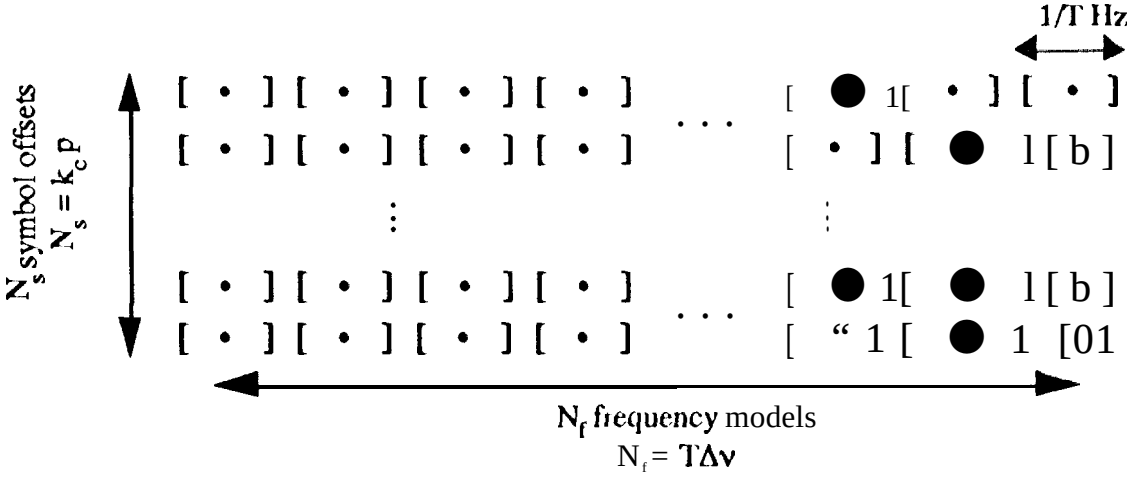


**Fig. 8 Search space for carrier signal with PN phase modulation. Each bracket pair represents the range of frequencies probed by a Fourier transform of N T-second signal x model points.**

Thus, at each model frequency, $N_s$ N-point Fourier transforms are performed. Assuming the Fourier transforms can be computed in real-time, $N_s$ x (NT) seconds are spent searching at each model frequency. Unfortunately, it is possible that this search algorithm would miss the signal entirely if the incoming signal's frequency is changing with time (due to unmodelled spacecraft-spacecraft relative acceleration and oscillator drift). For example, suppose the search is proceeding from higher to lower frequencies while the signal is increasing in frequency. Then if the signal moves into Cell (I,J) while we are searching frequency J and after we have already tried symbol offset I, we will end up searching the entire space without ever having tried a cell in which the signal was present.

The problem of a signal with moving frequency may be addressed by taking the following two steps: 1) set $k_f$ equal to 2, i.e. space the model frequencies by 1/2T Hz. Each Fourier transform of {signal x model} will still probe a region in frequency space of width 1/T Hz, but the region probed by adjacent frequency models will now overlap by 50%. 2) require that the change in signal frequency over a time $N_s$ x (NT) be smaller than (1/2T) Hz. Given an upper bound on the spacecraft-spacecraft relative acceleration and oscillator drift, this requirement places a constraint on the allowable values of the parameters $N_s$, N, and T. The impact of this and other constraints is discussed later. If this strategy is employed, the number of Fourier transforms required to search the entire 2-dimensional space is 2T Av $N_s$.

The signal detection procedure is very similar to the carrier detection method discussed earlier, Model signals are sequentially tested by mixing with the incoming signal and then Fourier transforming N points acquired over NT seconds. If a Fourier frequency bin has amplitude exceeding the detection threshold, then the same model is tested again. If a second detection occurs, it is assumed that the signal has been found and phase- and delay-lock-loop tracking is commenced. The mean time to signal acquisition is $\bar{T}_{ACQ} \approx NT^2$ Av $N_s$. The mean time to acquisition could be significantly reduced if the spacecraft hardware is capable of processing multiple model signals in parallel.

If the signal power is known, the amplitude threshold can be selected so that the probability of signal detection when signal is present, $P_{detect}$, is high (e.g. 99%), while the probability of a false alarm, $P_{false}$, is low (e.g. 1%). For a given probability of detection and probability of false alarm there is a functional relationship between the quantities $(P_t/N_0)T$ and N. For $P_{detect} = 0.99$, $P_{false} = 0.01$, and $k_c=2$ (symbol search proceeding in half-chip steps), the relationship between N and $(P_t/N_0)T$ is well-approximated by the following equation (see appendix): $(P_t/N_0)T = 43\ N^{-0.91}$

The contours in Fig. 9 are derived by combining the above two equations. As in the case of pure carrier detection, there are a number of constraints which restrict the allowable values of N, T, and NT.

<u>Constraint on NT arising from unmodelled spacecraft acceleration</u>. Earlier, we imposed the requirement that the change. in signal frequency over a time $N_s$ x (NT) be smaller than (1/2T) Hz.

$$\frac{d(f_0)}{dt} < \frac{1/2T}{N_s\,NT} \quad \Rightarrow \quad NT^2 < \frac{c}{2 f_0 N_s \delta a}$$

Here f. is the carrier frequency, c is the speed of light, and $\delta a$ is the unmodelled spacecraft acceleration. As in the case of simple carrier detection, it is also required that the time NT

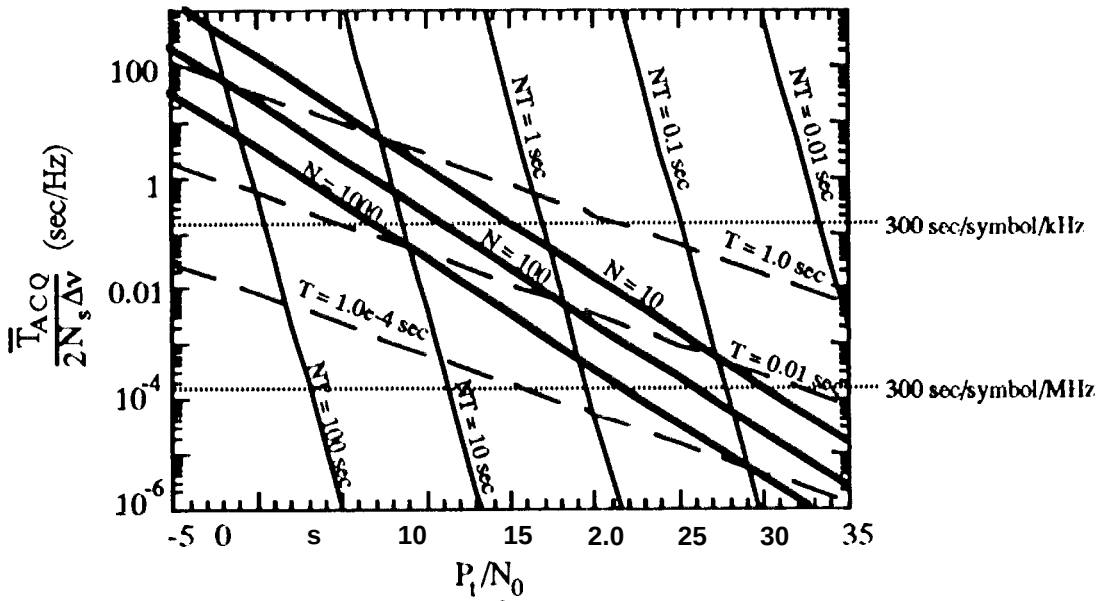


**Fig. 9** Relationships between $\bar{T}_{ACQ}/(2N_s\Delta\nu)$, N, T, and the $P_t/N_0$ requ red for signal acquisition with $P_{false} = 0.01$ and $P_{detect} = 0.99$.
— Ranging signal detection —

be small enough so that unmodelled spacecraft accelerations do not smear the signal over multiple Fourier frequency bins. Together, these two constraints are given by:

$$NT < \sqrt{\frac{c}{2\, f_0\, \delta a}} \times \mathrm{MIN}\left\{1, \sqrt{\frac{N}{N_s}}\right\} \tag{3}$$

Constraint on NT arising from unmodelled spacecraft velocity. It is required that the unmodelled spacecraft-spacecraft relative velocity be small enough so that the range does not change by more than 1/2 chip ($\tau_c/2$ seconds) over the NT seconds during which data are collected for a Fourier transform.

$$NT < \frac{c\tau_c}{2\,\delta v} \tag{4}$$

In this equation, $\delta v$ is the unmodelled spacecraft-spat.ccraft relative velocity.

Oscillator stability requirements. The constraints on oscillator stability are analogous to the constraints on NT arising from unmodelled spacecraft acceleration and velocity.

In analogy with the acceleration cons traint, it is required that the signal change by less than less than (1/2T) Hz over $N_s$ x (NT) seconds, and also that the carrier frequency not move through multiple Fourier frequency bins over the NT seconds during which data are acquired for the Fourier transform ($\Delta$freq. c 1/(2NT) over NT sec). Letting $\sigma_{y_i}(\tau)$ denote the -c-second Allan standard deviation of spacecraft i's oscillator,

$$\sqrt{\sigma_{y_1}^2(N_s NT) + \sigma_{y_2}^2(N_s NT)} < \frac{1}{2\, T\, f_0}$$

$$\sqrt{\sigma_{y_1}^2(NT) + \sigma_{y_2}^2(NT)} < \frac{1}{2\, f_0 NT} \tag{s}$$

In analogy with the velocity constraint, it is required that oscillator drift not introduce a delay of more than $\tau_c/2$ seconds over the NT seconds during which data are acquired for a Fourier transform. This con.. traint is looser than that imposed by the above equations for chip rates smaller than the carrier frequency (the usual case).

Example: Calculation of $P_t/N_0$ Required for Ranging Signal Acquisition. Suppose that ranging measurements are to be performed between a spacecraft approaching Mars and a beacon spacecraft on the planet's surface. The carrier frequency is S-Band, and the chipping rate is 1 MHz. The length of the PN code is 2047 symbols, corresponding to a two-way range ambiguity of 600 km. "lie ambiguity can be resolved via spacecraft position determinations resulting from routine Earth-based Doppler tracking of the two spacecraft.

The spacecraft are provided with a crude estimate of their relative velocity: 0.5 km/see, equivalent to 4000 Hz at S-Band. We assume that the spacecraft-spacecraft relative acceleration is not modelled. Until the approach spacecraft is within the sphere of influence of Mars (< 1 million km), the total relative acceleration of the. spacecraft and beacon is primarily due to Mars rotation, which imparts a 0.017 $m/sec^2$ acceleration to the beacon, Finally, we assume that the spacecraft hardware is capable of performing 1024-point Fourier transforms.

If the desired time to signal acquisition is S minutes, then the parameter constraints may be summarized as follows:

| *Constraint* | *Reason* |
|---|---|
| $\bar{T}_{ACQ}/2N_s\Delta\nu \lesssim$ 1 O-s sec/Hz | 5 min. acquisition, Av = 40001175 and $N_s$ = 4094 |
| N <1024 | Capability of FT chip on spacecraft |
| NT <0.03 $\sqrt{N}$ sec | Eq. (3) (unmodelled accel.) |
| NT < 0.3 sec | Eq. (4) (unmodelled velocity) |

All four constraints are satisfied in the unshaded region of Fig. 10 bounded by the contours N = 1024 and $\bar{T}_{ACQ}/2N_s\Delta\nu = 10^{-5}$ sec/Hz. The minimum $P_t/N_0$ satisfying the constraints is approximately 29 dB-Hz.

Eqs. (5) may now be applied to determine the oscillator stability requirements:

$\sigma_y$ (409 see) <2 x $10^{-6}$ see/see, $\sigma_y$ (O. 1 see) <2 x $10^{-9}$ see/see

These AlIan variances are easily met by non temperature-stabilim-d crystal Oscillator.

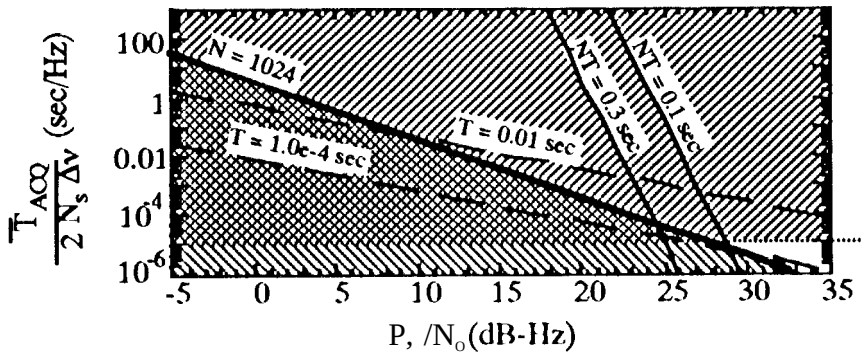


**Fig. 10 Given the constraints $\bar{T}_{ACQ}/2N_s\Delta\nu$ < 10-s and N < 1024, the minimum $P_t/N_0$ enabling reliable ranging signal detection is 29 dB-Hz**

Fig. 5 indicates that if both the lander and approach spacecraft are equipped with l-meter diameter antennas and mediocre receivers ($T_{rec}$ = 350 K), a 5 Watt S-Band signal is sufficient to enable 29 dB-Hz signal power to noise density ratio at spacecraft separations of millions of kilometers.

## RANGING MEASUREMENT PRECISION

To within a factor of order unity, the precision with which PN codes can be aligned with a delay lock loop is $1/\sqrt{2P_t/N_0 T_{dwell}}$, where $T_{dwell}$ is the integration time. The resulting ranging measurement precision is:

$$\varepsilon_\rho \text{ (meters)} \approx \frac{c\,\tau_c}{\sqrt{2P_t/N_0 T_{dwell}}}$$

The exact expression for the ranging measurement precision depends on details of the delay-lock-loop design. In practice, the best alignment precision that can be achieved is between 0.01 and 0.001 chips due to dispersion effects in the processing signal path.

The utility of ranging is to eliminate the unknown bias inherent in earlier phase (Doppler) measurements. Once this bias has been determined, range changes can be precisely tracked by measuring the carrier phase. The phase of the carrier can be recovered with precision of a fraction of an RF wavelength, even when the transmitted signal has modulation index of It/2 (fully suppressed carrier).

## ERROR COVARIANCE ANALYSIS

In this section, the navigational utility of *in situ* radio tracking is illustrated through some examples drawn from a hypothetical future Mars mission, in which a spacecraft approaching Mars acquires Doppler and ranging measurements from a Mars-orbiting communications relay satellite. Error covariance computations for a sequential estimation scheme were performed using approximate models of the approach spacecraft and relay satellite trajectories, and the Doppler and ranging measurement errors. This analysis was not designed to be an exhaustive treatment of the approach navigation problem, but merely to illustrate some of the more significant aspects of the use of *in situ* Doppler and ranging measurements in this type of application. It should be remembered that although the particular application discussed below refers to Mars, *in situ* radio tracking is also applicable to missions to the Moon and other target bodies where radio beacons or additional spacecraft may be used as navigation aids.

The error analysis was performed using model parameters summarized in Table 1. 'he approach spacecraft was assumed to move on a hyperbolic path with respect to Mars; except for the final hours prior to arrival at periapsis, this assumption leads to a trajectory that is essentially rectilinear and of constant velocity. To illustrate the effect of different approach velocities on navigation performance, two different values of asymptotic approach velocity were considered, representative of the. minimum and maximum possible values for low-energy bal list ic Earth-to-Mars transfer trajectories. The radius of closest approach chosen for this study (3417 km) yields a periapsis altitude of about 20 km, which is representative of trajectories leading to a direct entry and landing, or the initiation of an aerobraking maneuver for orbit insertion. The Mars-orbiting relay satellite was assumed to be in a circular orbit with a 12 hour period. The spacecraft acceleration process noise level used in this analysis is intended to account for the small, non-gravitational forces (e.g.

**Table 1**
**MARS** APPROACH NAVIGATION ERROR ANALYSIS PARAMETERS

| *Trajectory Parameter* | *Value* |
|---|---|
| Asymptotic approach velocity ($v_\infty$) | 3 or 6 km/sec |
| Radius of closest approach | 3417 km |
| Inclination of approach trajectory to Martian equator | + 15 deg |
| Mars relay satellite orbital period | 12hr |
| Mars relay satellite inclination | 0 deg |
| Spacecraft acceleration process noise (approach spacecraft and relay satellite) | 2 x $10^{-10}$ $m^2/sec^4/hr$ |
| A Priori *State Uncertainties (1σ)* | *Value* |
| Approach spacecraft epoch position | 100 km |
| Approach spacecraft epoch velocity | 1 m/s |
| Relay satellite epoch position | 3 km |
| Relay satellite epoch velocity | 0.1 m/s |
| *Doppler Measurement Parameter* | *Value* |
| Maximum acquisition range | $2 \times 10^6$ km |
| Additive random measurement noise | 4 mm (1σ) |
| Accumulative random measurement noise | 0.S8 $m^2/hr$ |
| Frequency drift stability | 0.3 mm/s (1σ, *a priori)* |
| Carrier phase bias uncertainty | 100 km (1 σ, *a priori)* |
| *Ranging Measurement Parameter* | *Value* |
| Maximum acquisition range | $8 \times 10^5$ km |
| Additive random measurement noise | 5 m (1σ) |
| Range bias uncertainty | 15 m (1σ) |

solar radiation pressure mismodelling, gas leaks from valves and pressurized tanks) that act on an interplanetary spacecraft.

The navigational utility of both one-way integrated Doppler measurements and two-way ranging measurements has been investigated. Integrated Doppler data are effectively a measurement of the accumulative change in the spacecraft-to-spacecraft range over the contact period, As shown by the parameters given in Table 1, integrated Doppler provides a highly precise measurement of range, but with a large constant bias, The frequency drift uncertainty assumed for the Doppler measurements is representative of oscillator stability on the order of 10-12 see/see. Two-way ranging measurements are much less precise than Doppler measurements, but provide an accurate measure of the spacecraft-spacecraft separation (Table 1). &described earlier, acquisition of a ranging signal requires a more extensive. search than simple carrier signal acquisition. For fixed assumptions about the

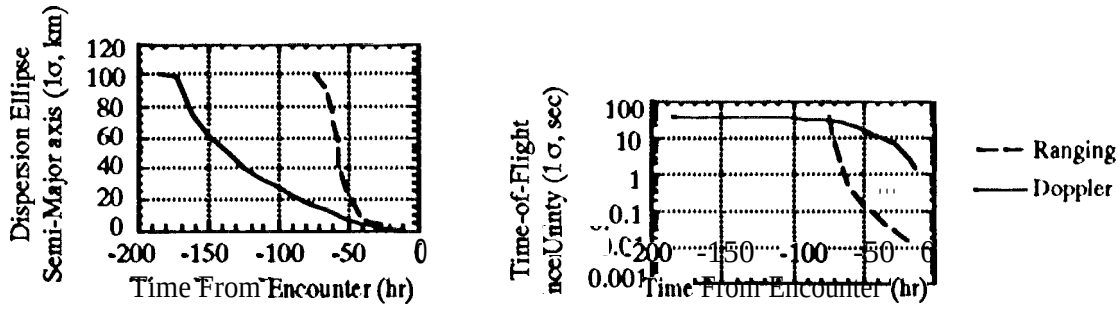


(a) **Aim-Point Uncertainty** (b) **Linearized Time-of-Flight Uncertainty**

**Fig. 11 Mars approach navigation dispersions ($v_\infty$ = 3 km/s)**

**spacecraft** on-board computing **resources** and the desired mean-time-to-signal- acquisition, the requirement on $P_t/N_0$ is higher to support ranging acquisition. **As** a result, the acquisition range for ranging data is **considerably** smaller than for Doppler data.

The results of the error **covariance** analysis are summarized in **Figs.** 11 and **12.** These figures show the uncertainties in the approach spacecraft **encounter** coordinates as a function of time prior to arrival, expressed in an aiming plane (B-plane.) coordinate system.* Fig. 11 shows the semi-major axis **of** the aiming plane dispersion ellipse and the **linearized** time-of-flight uncertainty (position uncertainty in the ***S*** unit direction divided by $v_\infty$) for an approach velocity of 3 km/see, while Fig. 12 shows the same two quantities for an approach velocity of 6 km/see. Note that in practice, delay-lock-loop tracking of a **PN-**modulated carrier **signal** enables **recovery** of the carrier phase, thus enabling simultaneous acquisition of ranging and integrated Doppler measurements. However, **Figs.** 11 and 12 show the navigational uncertainties resulting from the use of either data type **independentl** y, in order to illustrate differences in the ability of the two data types to determine various components of the approach trajectory.

Both Fig... 11 and 12 **illustrate** a clear difference between Doppler and ranging performance: since ranging data provide a direct measurement of the spacecraft-spacecraft separation, the time-of-flight (which in this case is essentially the spacecraft range) **can** be

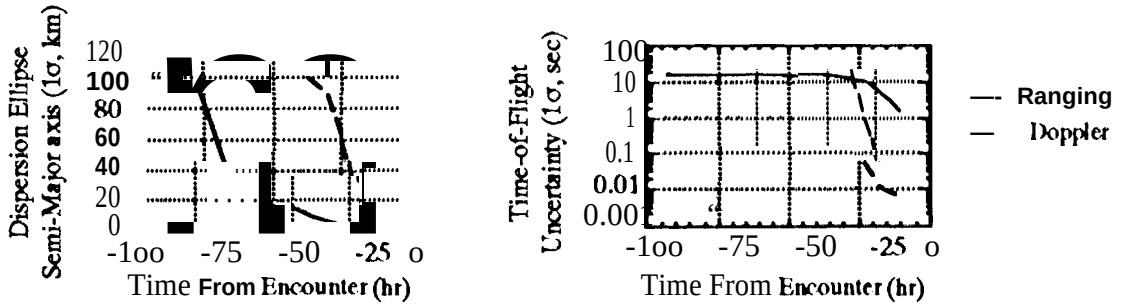


**(a) Aim-Point Uncertainty** **(b) Linearized Time-of-Flight Uncertainty**

**Fig. 12 Mars approach navigation dispersions ($v_\infty$ = 6 km/s)**

**' The aiming plane, or *B*-plane, coordinate system is defined by three unit vectors, S, *T, and* R; S is parallel to the incoming asymptote of the approach hyperbola, *T* is parallel to the Martian equatorial plane, and *R* completes an orthogonal triad with S and *T*. The aim point for a planetary encounter is defined by the miss vector, *B,* which lies in the *T-R* plane, and specifies where the point of closest approach would be if the target planet had no mass and did not deflect the spacecraft's flight path.**

very accurately determined immediately upon acquisition, In constrast, Doppler data can only measure this component of the flight path indirectly, and need to be collected for up to several days before sufficient information is obtained. This occurs because Doppler data depend upon the relative acceleration of the approach spacecraft and the relay satellite (which is inversely dependent upon their relative range) to determine the time-of-flight, Additional experimentation found that the approach spacecraft acceleration process noise was the principal factor limiting the integrated Doppler's ability to determine the time-of-flight.

Fig. 12 shows that when the approach velocity is relatively high, the. smaller acquisition distance associated with two-way ranging results in the aiming plane dispersion ellipse of the approach spacecraft remaining relatively large until about 15 hours prior to arrival. If a final maneuver is needed to correct the spacecraft's aim point, this implies that the maneuver may have to be performed very near the arrival point, with the ensuing risk that there may not be sufficient time remaining to redetermine the trajectory and correct any maneuver execution errors that might have occurred. Thus, if large approach velocities must be accommodated, early acquisition of Doppler followed by joint acquisition of Doppler and ranging data would be desirable.

## SUMMARY

The $P_r/N_0$ required for acquisition of carrier or ranging signals between two spacecraft is a function of a number of parameters, including *a priori* uncertainty in the spacecraft-spacecraft relative state, and the capabilities of the spacecraft processing hardware and software (e.g. the maximum number of points which can be Fourier transformed in real-time). Once these parameters are specified, one may calculate the maximum range at which a signal can be acquired, for a given set of assumptions about the spacecraft telecommunications systems. A.. an example, it has been shown that S-Band radiometric measurements between a Mars lander and Mars approach spacecraft equipped with 1-meter diameter antennas are feasible over distances of millions of kilometers. The analysis presented here can easily be applied to a wide variety of other mission scenarios.

To illustrate the utility of in-situ radiometric measurements between spacecraft, a covariance analysis was performed for the case of Doppler and ranging measurements between a Mars orbiter and a spacecraft on Mars approach, The results obtained are consistent with previous studies, and suggest that approach navigation accuracies of a few kilometers at Mars maybe obtained with either *in situ* Doppler or ranging measurements.

In the near-term, *in-situ* ranging and Doppler data between spacecraft would likely be relayed to Earth for navigation processing. Ultimately, on-board computing resources could be used to perform the navigation updates, enabling a near real-time *in-situ* navigation capability.

## ACKNOWLEDGMENT

The research described in this paper was carried out by the Jet Propulsion Laboratory, California Institute of Technology, under a contract with the National Aeronautics and Space Ministration.

## REFERENCES


1. A. S. Konopliv and L. J. Wood, 'High-Accuracy Mars Approach Navigation with Radio-Metric and Optical Data,' Paper AIAA-90-2907, AIAA/AAS Astrodynamics Conference, Portland, Oregon, August 20-22, 1990

2. S. W. Sheppard, D. P. Fuhry, and T. J. Brand, "Onboard Preaerocapture Navigation Performance at Mars,' Paper AAS91-119, AAS/AIAA Spaceflight Mechanics Meeting, Houston, Texas, February 11-13, 1991

3. S, W, Thurman and J. A. Estefan, "Mars Approach Navigation Using Doppler and Range Measurements to Surface Beacons and Orbiting Spacecraft,' Paper AAS 91-118, AAS/AIAA Spaceflight Mechanics Meeting, Houston, Texas, February 11-13, 1991

4. S. W. Thurman and S. E. Matousek, "Trajectory and Navigation System Design for Robotic and Piloted Missions to Mars,' *The Telecommunications and Data Acquisition Progress Report 42-107,* Vol. July-September 1991, Jet Propulsion Laboratory, Pasadena, California, pp. 113-131, November 15, 1991

5. M. K. Simon, J. K. Omura, R. A. Scholtz, and B. K. Levitt, *Spread Spectrum Communications, Volume III*, Computer Science Press, Rockville, Maryland, 1989

6. R. Dixon, *Spread Spectrum System,* John Wiley and Sons, New York, 1984

7. S. A. Stephens, 'An analysis of FFT tone acquisition', JPL interoffice Memorandum 335.1-92-14 (internal document), May 14, 1992

## APPENDIX

As described in the text, the carrier detection strategy involves looking for Fourier resolution bins whose amplitude exceeds a threshold level. The detection threshold parameter, $\xi$, is selected such that the probability that the amplitude of the signal plus noise exceeds $\xi$ x {expected signal amplitude} is 0.995. The probability of two consecutive signal detections when the signal is present, which shall be referred to as $P_{detect}$, is then 0.99. Calculation of the detection threshold must take into account signal amplitude losses resulting from two effects: 1) If the signal lies within the 1/T Hz range probed by the Fourier transform, it may differ from the model by up to 1/2T Hz. Thus, each T-second average of the signal x model phasor suffers amplitude loss because the phasor is not completely "stopped", 2) the signal will in general lie somewhere between Fourier resolution bins, so that the amplitude of the Fourier bin closest to the signal can be smaller than the true signal strength. The first effect can be ameliorated by discarding the Fourier resolution bins which lie toward the edges of the 1/T Hz frequency span, at the cost of increasing the number of Fourier transforms required to cover the entire search space of $\Delta\nu$ Hz. The fraction of Fourier resolution bins retained is referred to as $\chi$. The second effect can be reduced by "oversampling", i.e. padding the data points with additional zeros, to decrease the frequency bin size of the Fourier transform. The degree of oversampling is described by a quantity, $\kappa$, which is equal to N/(N+the number of padded zeros). Note that decreasing $\kappa$ allows finer sampling of the Fourier transform at the cost of requiring increased computation (i.e. Fourier transforming a larger number of data points).

In Ref. 7, it is argued that a reasonable selection of $\chi$ and $\kappa$, from the standpoint of minimizing acquisition time, is $\chi = 1$ and k = 1/2. Given this choice of $\chi$ and $\kappa$, it can be shown that the detection threshold parameter, $\xi$, is given by the following formula[3]:

$$0.995 = 2\int_{-1/2}^{1/2} du \int_{-1/4}^{1/4} dw\, (SNR_v)^2\, e\text{-es}^{(\alpha\, SNR_v)^2} \int_{\xi}^{\infty} dr\, r\, e^{-0.5\, r^2 SNR_v^2}\, I_0(\alpha\, r\, SNR_v^2)$$

where $\alpha = \frac{\sin(\pi u)}{\pi u} \times \frac{\sin(\pi w)}{\pi w}$.

$I_0$ is the 0th order modified Bessel function, and

$SNR_v$ is the voltage signal-to-noise. ratio over NT seconds, = $\sqrt{2\, P_t/N_0\, NT}$

The probability that the noise amplitude in a given frequency bin exceeds $\xi$ $SNR_v$ is $\exp(-0.5\,(\xi\, SNR_v)^2)$. Thus, the probability, $P_{false}$, that the noise amplitude exceeds $\xi$ $SNR_v$ in at least one of N frequency bins is:

$$P_{false} = 1 - (1 - \exp(-0.5\,(\xi\, SNR_v)^2))^N$$

The first equation allows numerical calculation of $\xi$ as a function of $SNR_v$. Now if we require that $P_{false} = 0.01$, then the second equation allows calculation of N as a function of $SNR_v$. But since $SNR_v = \sqrt{2\, P_t/N_0\, NT}$, N may then be calculated as a function of $(P_t/N_0)T$. Over the range $6 < SNR_v < 12$, $(P_t/N_0)T \approx 29\, N^{-0.92}$.

in the case of detection of a PN-modulated carrier, the calculation is analogous, but $SNR_v$ must be scaled by $(1 - 1/(2k_c))$, where $1/k_c$ chips is the model symbol offset step size. This factor accounts for the $SNR_v$ loss during detection, due to the fact that the best alignment of the model and signal sequences may be off by as much as $1/2k_c$ chips. If the search is conducted in ha if-chip increments ($k_c$=2) and we desire $P_{detect} = 0.99$ and $P_{false}$= 0.01, then the relationship between $(P_t/N_0)T$ and N is: $(P_t/N_0)T \approx 43\, N^{-0.91}$.